

RISER DESIGN IN FOAM FRACTIONATION

P.J. Martin*, M. Swain and R.C. Darton

Department of Engineering Science, University of Oxford, Parks Rd, Oxford OX1 3PJ, UK

*E-mail: peter.martin@eng.ox.ac.uk

The growth of biotechnology has led to renewed interest in the possibility of enriching valuable bioproducts using foam fractionation. This is a separation process in which surface active molecules are separated from a solution by sparging through bubbles of gas. Adsorption of such molecules at the gas/liquid interface causes enrichment in the foam formed above the liquid pool. Previous work has shown that liquid flow and mixing in the foam riser are crucial features determining the degree of separation. Theoretical considerations suggest that diffusion in the Plateau borders of the rising foam is the principal cause of mass transfer between the rising liquid and the reflux. This diffusion is one element of the well-known Taylor dispersion, and it enhances enrichment in the riser. An experimental study has measured the velocities of the counterflowing streams within a riser, and the axial dispersion. Fitted dispersivity values are similar to those previously published. Further modelling of the dispersion processes will enable these experimental values to be related to the enrichment within the riser, enabling confident design and control of foam fractionation columns.

KEYWORDS: foam fractionation, adsorption, riser, foam, dispersion, mixing

INTRODUCTION

Foam fractionation was developed in the 1960s as a process for separating surface active agents (surfactants) from solution. The process can also be used to separate a variety of other molecules which bind to surfactants. Lemlich (1972a) provides an overview of its development and context.

Batch foam fractionation, shown in Figure 1, consists of a pool of surfactant solution in a vertical column through which gas is sparged. Surfactant molecules adsorb to the gas-liquid interface as bubbles rise through the pool, making a foam which flows up the riser. Interstitial liquid drains from the films between the bubbles (lamellae) into the junctions of the lamellae (Plateau borders), and drains down the network of Plateau borders, which are interconnected at vertices, back into the pool. Foam collected from the top of this column contains gas, bubble surfaces onto which surfactant is adsorbed, and some of the initial solution in the interstices. Thus, collapsing the foam and releasing the gas results in surfactant solution (foamate) greater in concentration than the initial solution. Figure 1 shows a mechanical paddle foam breaker, but other technologies also exist (Barigou, 2001). The enrichment is the factor by which the initial solution concentration is increased in the foamate, which can often be several orders of magnitude.

The growth of biotechnology has revived interest in the use of foam fractionation as a product enrichment stage. The high value of some bioproducts demands optimal foam

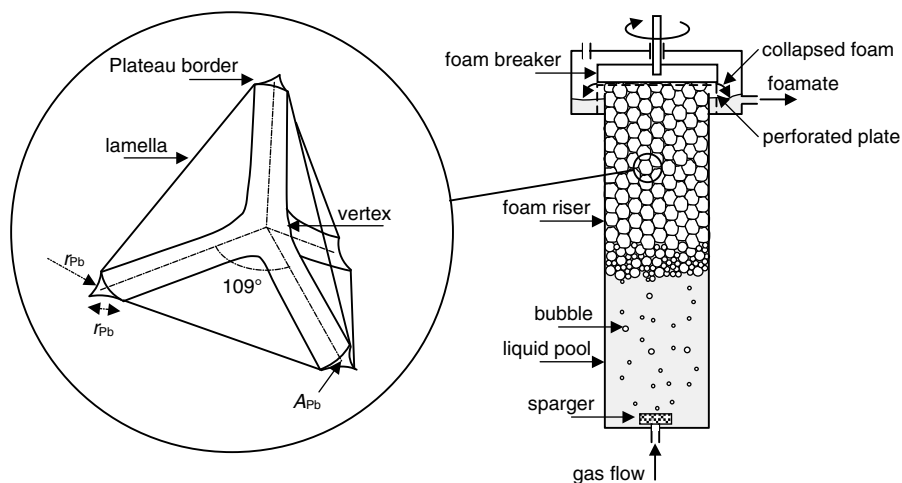


Figure 1. Batch foam fractionation, with schematic detail of foam structure

fractionation performance, requiring advanced features such as reflux, multiple stages and continuous operation. This paper presents a theoretical model, and novel experimental measurements of foam dispersion. Our objective is to be able to design and operate better equipment, based on knowledge of the actual mechanisms occurring.

MODELLING COUNTERFLOW FOAM FRACTIONATION PROCESS OUTLINE

As the batch separation shown in Figure 1 progresses, enriched surfactant is collected as foamate. Eventually there will be insufficient surfactant to create a stable foam, since the concentration in both the liquid pool and the foamate decreases with time, a characteristic typical of batch fractionation. Figure 2 illustrates two possible modes of continuous operation, following the outline proposed by Lemlich (1972b). The simple mode introduces a continuous flow through the liquid pool; separation is achieved by the same adsorption and drainage process as in batch operation. The counterflow mode feeds a reflux of enriched foamate back into the riser. The enriched solution flows down the network of Plateau borders and vertices and mixes with the original interstitial solution. The mixing of the enriched falling stream with the rising stream increases the concentration of the rising stream, thus increasing the enrichment over the riser. The counterflow mode is usually operated such that the volumetric fraction of liquid in the foam (holdup) is constant (except near the bottom) and thus the falling stream flow rate is equal to the reflux. Other aspects of foam behaviour, such as coalescence and coarsening, are assumed to be negligible.

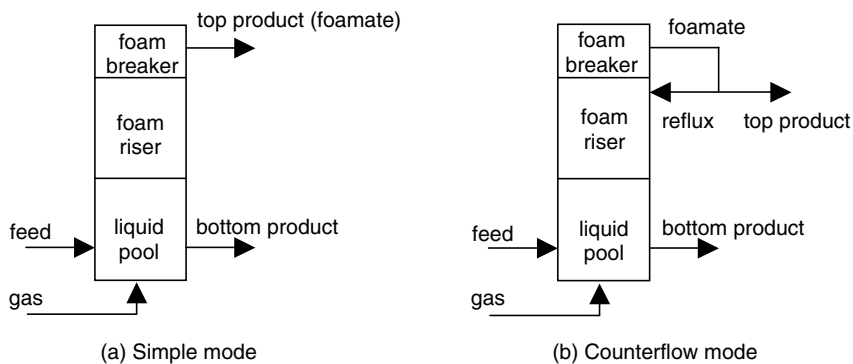


Figure 2. Modes of continuous enriching foam fractionation operation (Lemlich, 1972b)

Figure 3 shows how surfactant is transported in the riser by three processes. (i) The flow of surfactant adsorbed on to the interface, ΓA , where Γ is the surface concentration and A is the interfacial area flow rate up the riser. The surface concentration is in equilibrium with the interstitial liquid, but often reaches a constant saturation level when the interstitial solution is over the critical micelle concentration (CMC) and in this paper Γ is treated as a constant. (ii) The flow of surfactant in the rising stream, $V_0 c_0$, where V_0 is the rising stream flow rate and c_0 is the surfactant concentration in the rising stream. (iii) The flow of surfactant in the falling stream, $V_0 c_1$, where the flow rate V_0 is the same as in the rising stream because the riser is operating at total reflux in this case. c_1 is the surfactant concentration in the falling stream.

Figure 3(a) illustrates the mixing stage approach to modelling the riser (Lemlich, 1972b). Over the height of a mixing stage the streams are perfectly mixed, resulting in exit streams of equal concentration, $c_{0n} = c_{1n}$. Each subsequent stage increases the

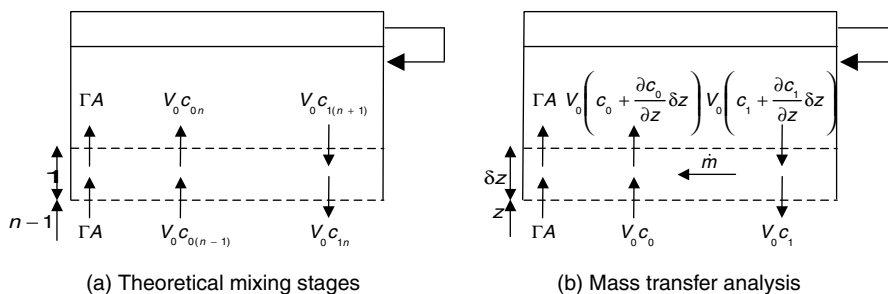


Figure 3. Analysis of top section of riser for counterflow mode operating with total reflux

mass transfer from the falling stream to the rising stream, so that the greater the number of stages the greater the enrichment. The total number of mixing stages in a riser N is

$$N = \int_{c_{0\text{bottom}}}^{c_{0\text{top}}} \frac{dc_{0n}}{c_{0n} - c_{0(n-1)}} \quad (1)$$

Darton *et al.* (2004) found between 4 and 10 mixing stages in a riser 140 mm tall. The mixing stage approach offers a useful way of establishing design correlations, but is inherently empirical.

Figure 3(b) illustrates the physical processes occurring over an element of the riser height, z . Within this element the change in concentration in the rising and falling streams is represented by a mass transfer of surfactant at rate \dot{m} . A model of mixing between the rising and falling streams is required in order to estimate this mass transfer rate, which requires consideration of the dispersion processes occurring in the foam.

DISPERSION WITHIN FOAMS

Work by Stevenson *et al.* (2003) and Lee *et al.* (2005) has addressed the dispersion processes occurring within foams. Stevenson *et al.* injected a fluorescent tracer into a foam, and tracked its motion, although they do not report values of dispersivity. Lee *et al.* contend that the introduction of excess liquid volume with the tracer will lead to capillary suction within the foam, masking the dispersion processes which are of interest. They avoided this problem by injecting a tracer of suspended particles or dye into the flow of a forced drainage experiment. This introduces no excess liquid volume, thus avoiding effects of capillary suction.

Lee *et al.* discuss four possible modes of dispersion within a foam: (i) geometrical dispersion as the flow makes its way through the many Plateau border paths, (ii) mixing at the vertices, (iii) convective dispersion due to the velocity profile across Plateau borders, and (iv) diffusive dispersion due to the concentration profiles across Plateau borders. They argue that modes (i) and (iii) would lead to sharp increases in concentration as the flow front passes a point on the riser, as opposed to modes (ii) and (iv) which would lead to Gaussian distributions. They report measurements of Gaussian profiles and thus conclude that modes (i) and (iii) are negligible. Furthermore, they argue that mode (ii) will cause the dispersion to be dependent on bubble radius, whereas mode (iv) will not. They report measurements of diffusivity which are independent of bubble radius, and thus conclude that mode (ii) is also negligible. Thus mode (iv), diffusive dispersion due to the concentration profile in Plateau borders, is the dominant mode of dispersion in foams, they conclude. Further work will be required for these results to be verified.

Dispersion modes which tend to mix randomly in an axial direction lead to the concentration profile being of the well-known form for open systems,

$$\hat{c} = \frac{1}{\sqrt{4D_A \pi t}} \exp\left(-\frac{(z - v_c t)^2}{4D_A t}\right) \quad (2)$$

where \hat{c} is the normalised concentration, D_A is an axial dispersion coefficient, t is the time since the tracer was introduced, z is the distance along the riser from the point where the tracer was introduced, and v_c is the average liquid velocity relative to the riser wall.

Figure 4 shows the cross section of a Plateau border which, for illustrative purposes, is considered to be vertically aligned and of circular cross section with radius R . A parabolic velocity profile, v , is shown over the radial direction, r , of the channel for the case of counterflow foam fractionation. At total reflux the rising stream flow rate is equal to the falling stream flow rate (there is no net liquid flow up or down). Thus, the average liquid velocity relative to the bubbles (this velocity is *downwards*), v_l , is equal in magnitude to the upwards velocity of the bubbles relative to the riser, v_b , given by,

$$v_b = \frac{G}{(1 - \phi)A_{col}} \approx \frac{G}{A_{col}} \quad (3)$$

where G is the volumetric gas flow rate, A_{col} is the riser cross-sectional area and ϕ is the liquid holdup. With this arrangement, both the average velocity of the rising stream, $v_{c,r}$, and the average velocity of the falling stream, $v_{c,f}$, will be equal in magnitude to half the average liquid velocity relative to the bubbles.

Diffusion due to the concentration profiles across Plateau borders would appear to be the principle mass transfer process in this counterflow arrangement. Diffusion across the velocity profile of a fluid flowing in a pipe is a component of Taylor dispersion (Taylor, 1953), which *reduces* axial dispersivity. In our case this diffusive dispersion serves to mix surfactant between “rising” and “falling” liquid streams in the Plateau Borders, and enhances enrichment. We note that the axial dispersivity in Taylor dispersion varies inversely with the molecular diffusivity. If Lee *et al.*'s (2005) conclusion that there is negligible mixing at the vertices can be confirmed, then an approximate physical model of foam fractionation may be developed based on an equation of the form,

$$\dot{m} = kA_r \frac{(c_1 - c_0)}{r_{pb}} \quad (4)$$

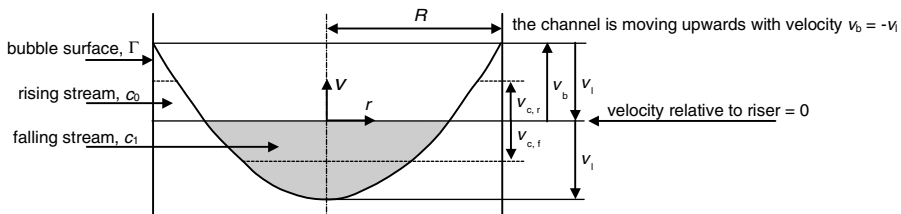


Figure 4. Plateau border flows at total reflux represented as parabolic flow in a rising circular channel

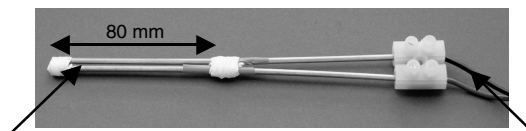
where the mass transfer rate is proportional to the product of the transfer area within the Plateau borders in the riser element, A_t , and a characteristic concentration gradient $(c_1 - c_0)/r_{pb}$. Plateau border geometry is such that the radius of curvature, r_{pb} , is equal to the width (see Figure 1). The coefficient k will be a function of the surfactant diffusivity. The results of Lee *et al.* are significant in that if just one mode of dispersion is dominant, then values of D_A obtained by fitting Equation (2) to experimental data may be used to deduce values of k . The situation would be more complex if significant dispersion also occurs at the vertices.

EXPERIMENTAL METHODS

The general approach of Stevenson *et al.* (2003) was employed to measure the dispersivity in foams over a range of gas flow rates. A glass foam fractionation column of circular cross section (Figure 6) was operated in counterflow mode, nominally at total reflux. A glass cylinder was attached 20 mm below the top of the riser to allow for an overflow pool to form. A glass cap allowed foam to flow through holes in the top towards a rotating paddle foam breaker, and allowed liquid to flow through holes at the bottom, over a weir, and back into the riser. Air was sparged through a sintered glass block to create the bubbles. Sampling points were spaced at 50 mm centres on the side of the riser.

Aqueous cetylpyridinium chloride (CPC) solution was pumped through the liquid pool in order to maintain a constant concentration of 0.35 mM, and air was sparged at rates between 0.4 and 0.7 L min⁻¹. CPC has a CMC of 1 mM and the saturated surface excess has been calculated at 2.64×10^{-6} mol m⁻² (Aubourg *et al.*, 2000). The pool at the top of the column was filled with 0.35 mM solution prior to operation. The column was left to run for approximately 40 minutes, by which time measurements of concentration within the riser suggested reasonably steady operation had been achieved.

Stevenson *et al.*'s (2003) method of injecting a fluorescent tracer was attempted, but the brightness of tracer fluorescence within the riser was too low to allow observation. Instead a 50 ml volume of 50 mM salt solution was injected into the centre of the riser over approximately 3 s. Conductivity probes, illustrated in Figure 5, were used to measure the conductivity of the foam. The 5 mm diameter stainless steel conductors were held 2 mm apart and spanned the width of the riser. It was assumed that the conductivity over the probes was proportional to the mean salt concentration of the foam between the conductors.



Two stainless steel rods 2mm apart which span column diameter

Connected to conductivity meter

Figure 5. Conductivity probe

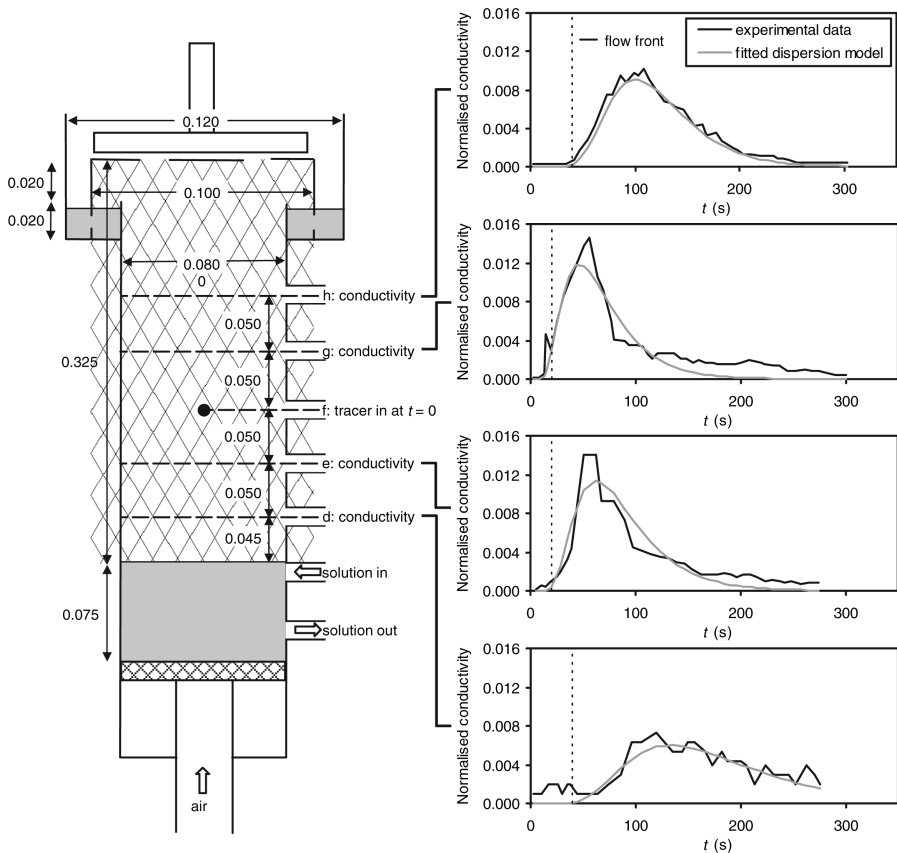


Figure 6. Column arrangement for dispersion experiments (with dimensions in m) showing conductivity profiles for $G = 0.71/\text{min}$

The salt solution was injected at position f (see Figure 6), 14.5 mm above the liquid pool surface, and the conductivity was measured 50 and 100 mm above and below this point. The response at sampling points g and h (above the injection point) were measured in one experiment, while the response at sampling points d and e (below the injection point) were both measured in a separate experiment.

The conductivity readings were adjusted to account for the baseline foam conductivity, and then the profiles were normalised to have unit area. The average stream velocities, $v_{c,r}$ and $v_{c,f}$, and the axial dispersivity, D_A , were deduced by fitting these profiles with equation (2) using the least squares method.

RESULTS AND DISCUSSION

A stable foam was formed in the riser with bubbles observed to be approximately 0.5 mm in diameter. These bubbles proved difficult to break, causing a thick secondary foamate to form around the foam breaker. Furthermore, the liquid level in the pool of foamate at the top of the column, which was intended to flow over the weir as reflux, tended to fall throughout the experiment. Pearson (2004) reported similar behaviour, and it is presumed to be due to capillary suction. Consequently, the target total reflux condition was only approximately achieved. Suitable conditions were achieved for dispersion experiments to be conducted, but reliable mass balances of surfactant over the column were not possible. The liquid holdup was measured to be approximately 0.1 immediately above the pool, which dropped to a constant value of approximately 0.02 at a foam height of 100 mm and above.

Normalised conductivity measurements are shown in Figure 6. A delay was observed before any conductivity was measured, which corresponded to the expected arrival of the flow front given by $v_1/\Delta z$. The counterflow effect is clearly demonstrated. In effect, both the rising and falling streams were dosed with tracer at the same point in space and time. The flow of the tracer along each stream in opposite directions relative to the riser is apparent with dispersion increasing as the flow progresses.

Fitted values of dispersivity and counterflow velocity ($v_c = |v_{c,f}| = |v_{c,r}|$) are presented in Figure 7. Experimental and fitting inaccuracies lead to significant scatter within the data, although it is not much more than that reported by Lee *et al.* (2005), whose experiments were more conveniently designed. Repeat experiments yielded fitted parameters which were typically within 10% of previous values.

Figure 7(a) shows that the fitted dispersivities increased as the average liquid velocity relative to the bubbles increased. Lee *et al.* (2005) reported dispersivities in their

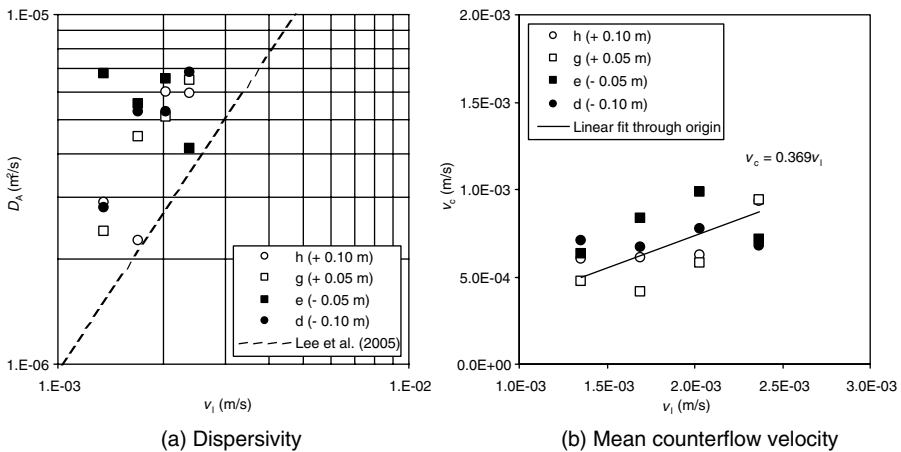


Figure 7. Plateau border flow characteristics against mean liquid velocity

forced drainage experiments increasing in a power law relationship from 5×10^{-6} to $8 \times 10^{-5} \text{ m}^2 \text{ s}^{-1}$ as the average liquid velocity increased from 0.003 m s^{-1} to 0.02 m s^{-1} ; their correlation is shown in Figure 7(a). The fitted dispersivities are in broad agreement with those of Lee *et al.*, the slightly higher values perhaps being a consequence of capillary suction effects. Their forced drainage arrangement did not create the counter flow used in our experiments, so close agreement between the dispersivities is not necessarily expected.

Figure 7(b) shows that the fitted counterflow velocities were comparable in both rising and falling streams. This indicates that, on average, the rising and falling streams occupy equal proportions of the Plateau border cross-sectional area. The counterflow velocity was found to increase linearly with the average liquid velocity. The trend displays a gradient of 0.369 when fitted through the origin by the least squares method. The flow scheme suggested in Figure 4 for parabolic flow in a circular channel gave the counterflow velocity to be half the average liquid velocity. This scheme was chosen for illustrative convenience, so the agreement is reasonable. More detailed consideration of actual Plateau border geometry and velocity profiles might arrive at a gradient closer to that found experimentally.

These experiments show that the axial dispersion and average velocity of both rising and falling streams can be measured in a counterflow foam fractionation riser. Improved experimental techniques, particularly with respect to the foam breaking mechanism and the design of the top liquid pool, will enable more accurate results to be obtained. Further theoretical consideration of the dispersion modes is required before fitted dispersion coefficients can be related to the mass transfer processes between the counterflow streams, but once achieved, a physical model of foam fractionation column design and operation will be obtainable.

CONCLUSIONS

We conclude that diffusion in the Plateau borders appears to be the principal cause of mass transfer between the rising liquid and the reflux in the foam riser. This diffusion is one element of the well-known Taylor dispersion, and it enhances enrichment in the riser. It has been shown to be possible to measure the axial dispersivity and the average velocities of the counterflowing streams in a riser. Both of these broadly followed the trends expected from other studies in the published literature. Mixing at vertices in the foam, and perhaps other mechanisms, require further investigation. Further theoretical work is also needed to incorporate this understanding in a model of the transfer processes in the riser, in order for us to achieve our goal of being able to design and operate better equipment.

ACKNOWLEDGEMENTS

The authors gratefully acknowledge the comments of Dr Stephen Neethling of Imperial College, UK, and Dr Paul Stevenson of the University of Newcastle, Australia.

REFERENCES

1. Aubourg, R., Bee, A., Cassaignon, S., Monticone, V., and Treiner, C. (2000) Adsorption Isotherms of Cetylpyridinium Chloride with Iron III Salts at Air/Water and Silica/Water Interfaces. *J. Colloid Interface Sci.* **230**, 298–305.
2. Barigou, M. (2001) Foam rupture by mechanical and vibrational methods. *Chem. Eng. Tech.*, **24**, 659–663.
3. Darton, R.C., Supino, S. and Sweeting, K. J. (2004) Development of a multistage foam fractionation column *Chem. Eng. and Proc.* **43**, 477–482
4. Lee, H.T., Neethling, S.J. and Cilliers, J.J. (2005) Particle and liquid dispersion in foams. *Colloids Surf., A*, **263**, 320–329.
5. Lemlich, R. (1972a) *Adsorptive bubble separation techniques*. Academic Press, New York, USA.
6. Lemlich, R. (1972b) Principles of foam fractionation and drainage. In *Adsorptive bubble separation techniques*, ed. R. Lemlich, pp. 33–51. Academic Press, New York, USA.
7. Pearson, R. (2004) *Foam fractionation*. Part II Project Report, Dept. of Eng. Sci., University of Oxford, UK.
8. Stevenson, P., Sullivan, S.P. and Jameson, G.J. (2003) Short-time tracer dispersion in a two-dimensional rising froth. *Chem. Eng. Sci.*, **58**, 5025–5043.
9. Taylor, G.I. (1953) Dispersion of soluble matter in solvent flowing slowly through a tube. *Proc. Roy. Soc. Lond.* **A219** 186–203.
10. Teipel, U. and Aksel, N. (2001) Adsorption behaviour of nonionic surfactants studied by drop volume technique. *Chem. Eng. Tech.*, **24**, 393–400.